

## Starburst Dendrimers. 5. Molecular Shape Control

Adel M. Naylor and William A. Goddard III\*

Contribution No. 7786, Arthur Amos Noyes Laboratory of  
Chemical Physics, California Institute of  
Technology, Pasadena, California 91125

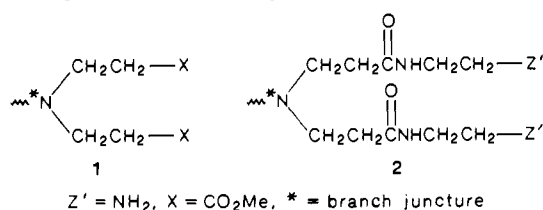
Garry E. Kiefer and Donald A. Tomalia\*

Functional Polymers Research  
Dow Chemical U.S.A., Midland, Michigan 48674

Received June 13, 1988

The recently reported "starburst dendrimer"<sup>1,2</sup> and "arborol"<sup>3</sup> systems provide unimolecular prototypes that allow for both endo-receptor and exo-supramolecular controlled molecular morphogenesis.<sup>9</sup> This present communication describes the use of molecular simulation and reiterative generation development as a means for predicting and controlling molecular size and topology.

In a previous communication,<sup>2</sup> where the initiator core (I) = NH<sub>3</sub> and the interior branch segments are  $\beta$ -alanine units such as **2**, it was presumed that these symmetrical junctured dendrimers



were expanding three dimensionally to produce regular spheroids as a function of generation (see Figure 1). Detailed experimental structural data have not been available on these materials due to the fractal nature of the polymers (which leads to disorder in the spatial configuration from dendrimer to dendrimer and hence no long-range order for X-ray diffraction). Consequently, in order to provide information on the overall shape of these dendrimers and on the presence and character of internal guest/host sites, we carried out molecular mechanics simulations of generations 1-7.<sup>4</sup>

The calculations used the AMBER force field<sup>5</sup> with the POLYGRAF molecular simulation programs.<sup>6</sup> These simulations indicate a dramatic change in morphology with generation, as indicated in Table I. Generations 1-3 are highly asymmetric ( $I_z/I_x = 4.4-2.7$ ), whereas generations 5-7 are nearly spherical ( $I_z/I_x = 1.3$ ), with the transition between the two forms ( $I_z/I_x = 1.7$ ) occurring at generation 4. We find the average structures for the early generations to be very open, domed shapes, as shown in Figure 2. The latter generations are more dense, spheroid-like topologies (Figure 2c) with solvent-filled interior hollows connected by channels that run the entire length of the macromolecule (Figure 2d). Generations 4-7 seem quite capable of encapsulating host molecules.

To experimentally investigate both the morphological changes as a function of generation and the predicted internal voids in the higher generation dendrimers, we carried out NMR studies of

(1) Tomalia, D. A.; Baker, H.; Dewald, J.; Hall, M.; Kallos, G.; Martin, S.; Roeck, J.; Ryder, J.; Smith, P. *Polym. J. (Tokyo)* **1985**, *17*, 117-132; *Macromolecules* **1986**, *19*, 2466. Tomalia, D. A.; Berry, V.; Hall, M.; Hedstrand, D. M. *Macromolecules* **1987**, *20*, 1164. Hall, H.; Padias, A.; McConnell, R.; Tomalia, D. A. *J. Org. Chem.* **1987**, *52*, 5305. Tomalia, D. A.; Dewald, J. R. U.S. Patent 4 507 466, 1985; U.S. Patent 4 558 120, 1985; U.S. Patent 4 568 737, 1986; U.S. Patent 4 587 329, 1986; U.S. Patent 4 631 337, 1986; U.S. Patent 4 694 064, 1987.

(2) Tomalia, D. A.; Hall, M.; Hedstrand, D. M. *J. Am. Chem. Soc.* **1987**, *109*, 1601.

(3) Newkome, G. R.; Yao, Z.-q.; Baker, G. R.; Gupta, V. K. *J. Org. Chem.* **1985**, *50*, 2003. Newkome, G. R.; Yao, Z.-q.; Baker, G. R.; Gupta, V. K.; Russo, P. S.; Saunders, M. J. *J. Am. Chem. Soc.* **1986**, *108*, 849. Newkome, G. R.; Baker, G. R.; Saunders, J. J.; Russo, P. S.; Gupta, V. K.; Yao, Z.-q.; Miller, J. E.; Bouillion, K. *J. Chem. Soc., Chem. Commun.* **1986**, 752.

(4) Naylor, A. M.; Goddard III, W. A., manuscript in preparation.

(5) Weiner, S. J.; Kollman, P. A.; Case, D. A.; Singh, U. C.; Ghio, C.; Alagona, G.; Proteta, S., Jr.; Weiner, P. *J. Am. Chem. Soc.* **1984**, *106*, 765.

(6) BioDesign, Inc., Pasadena, CA 91101.

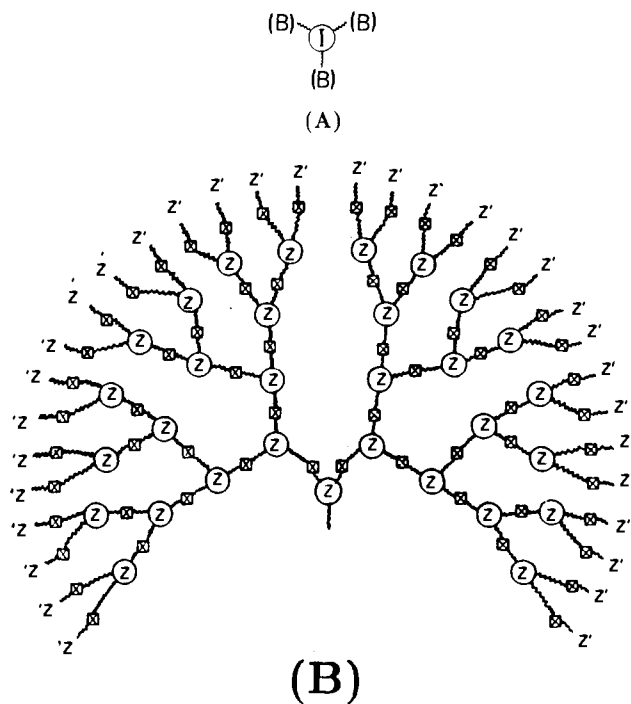


Figure 1. (A) Tridendron (tridirectional) dendrimer derived from ammonia where (I) = N and (B) are symmetrical branch junctured dendrons. (B) Monodendron (unidirectional) starburst branching patterns where  $\square$  = amide linkages are derived from **1**,  $\circ$  = branch junctures as designated in **1** and **2** advanced to generation = 6, and  $\text{Z}'$  is as designated in **2**.

Table I. Moments of Inertia for  $\beta$ -Alanine Starburst Dendrimers from Molecular Dynamics Simulation<sup>b</sup>

generation	$I_{\text{TOT}}^a$	% $I_x$	% $I_y$	% $I_z$	$I_z/I_x$
1	1.056	11.26	38.58	50.16	4.5
2	9.914	13.85	28.61	57.54	4.2
3	43.24	18.77	29.91	51.31	2.7
4	129.3	24.59	34.85	41.54	1.7
5	379.2	29.06	34.54	36.40	1.3
6	991.6	29.52	33.54	36.94	1.3
7	3131	29.88	31.16	38.96	1.3

<sup>a</sup>Units: daltons  $\times \text{\AA}^2$ . <sup>b</sup> $x, y,$  and  $z$  are the principal axes.

guest molecules in solution with carbomethoxy-terminated  $\beta$ -alanine dendrimers. By using the method of Menger and Jerkunica,<sup>7</sup> we found that 2,4-dichlorophenoxyacetic acid (**4**) and acetylsalicylic acid (**3**) exhibit behavior in the presence of dendrimer host molecules that supports the morphological changes predicted by the molecular simulations. For example, for generations 0.5-5.5, adding up to a limiting amount of  $X$  mmol of **3** or **4** to 1 mmol of the starburst carbomethoxy-terminated dendrimers (A) in CDCl<sub>3</sub> produced spin-lattice relaxation times ( $T_1$ 's) much lower than the values of **3** or **4** in solvent without dendrimer, where the new relaxation time decreases for generations 0.5-3.5, while remaining constant for generations 3.5 to 5.5 (see Table II and Figure 3). This maximum concentration  $X$  varies uniformly from 12 (generation 0.5) to 68 (generation 5.5). On the basis of these maximum concentrations, the stoichiometries for guest:host were shown to be  $\sim 4:1$  by weight and  $\sim 3:1$  based on a molar comparison of dendrimer guest carboxylic acid:interior tertiary nitrogen moieties for generations = 2.5-5.5. Exceeding this maximum concentration  $X$  leads to the appearance of a second relaxation time  $T_1$  characteristic of the guest molecules in bulk solvent phase in the absence of the dendrimeric hosts.

The  $T_1$ 's for the small organic molecules reach a minimum at dendrimer generation 3.5, while the simulations show a transition

(7) Menger, F. M.; Jerkunica, J. M. *J. Am. Chem. Soc.* **1978**, *100*, 688.

(8) Richards, F. *Ann. Rev. Biophys. Bioeng.* **1977**, *6*, 151.

(9) Lehr, J. M. *Angew. Chem., Int. Ed. Engl.* **1988**, *27*, 89.

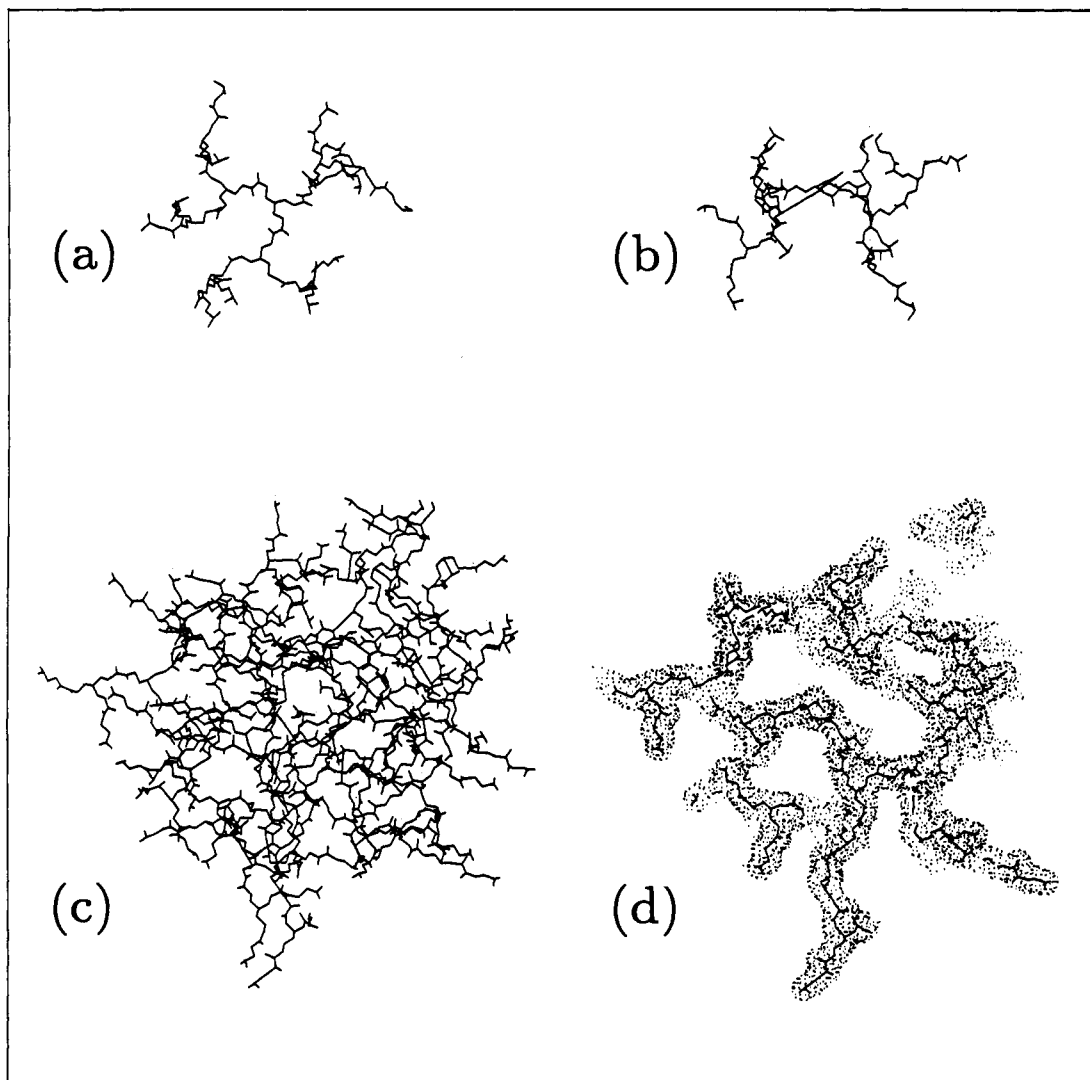


**Figure 2.** Orthogonal views of a  $\beta$ -alanine dendrimer. (a) and (b) illustrate the open, domed nature of the early generations (generation 3 shown), while (c) and (d) show the spherical nature of the late generations (generation 6 shown). In (d) the character of the solvent-filled void spaces is depicted with the use of solvent-accessible surfaces.<sup>8</sup>

**Table II.** Carbon-13 Spin-Lattice Relaxation ( $T_1$ , s) Measurements for Acetylsalicylic Acid (3) and 2,4-Dichlorophenoxyacetic Acid (4) in the Presence of Dendrimers (A) Where Terminal Groups are Designated as in 1 with X =  $-\text{CO}_2\text{Me}$

dendrimer generation	designated carbons					
	guest molecule (3)			guest molecule (4)		
	3	5	6	3	5	6
	$1.58 \pm 0.04$ (132.27) <sup>a</sup>	$1.30 \pm 0.03$ (134.54)	$1.76 \pm 0.06$ (123.81)	$1.66 \pm 0.10$ (130.41)	$2.70 \pm 0.45$ (127.66)	1.6 (114.15)
0.5	$0.82 \pm 0.01$ (131.67)	$0.60 \pm 0.01$ (133.08)	$0.81 \pm 0.01$ (123.23)	$0.74 \pm 0.02$ (129.67)	$0.89 \pm 0.01$ (127.28)	$0.74 \pm 0.02$ (114.48)
1.5	$0.34 \pm 0.01$ (131.43)	$0.30 \pm 0.01$ (132.41)	$0.37 \pm 0.02$ (122.87)	$0.47 \pm 0.004$ (129.70)	$0.57 \pm 0.01$ (127.38)	$0.049 \pm 0.02$ (114.58)
2.5	$0.26 \pm 0.01$ (131.63)	$0.24 \pm 0.01$ (132.52)	$0.27 \pm 0.01$ (123.07)	$0.38 \pm 0.004$ (129.79)	$0.43 \pm 0.01$ (127.54)	$0.35 \pm 0.02$ (114.78)
3.5	$0.22 \pm 0.02$ (131.26)	$0.22 \pm 0.02$ (132.13)	$0.22 \pm 0.01$ (122.76)	$0.34 \pm 0.01$ (128.64)	$0.38 \pm 0.01$ (127.41)	$0.35 \pm 0.01$ (114.66)
4.5	$0.23 \pm 0.01$ (131.42)	$0.25 \pm 0.01$ (132.28)	$0.27 \pm 0.02$ (122.92)	$0.40 \pm 0.01$ (129.57)	$0.39 \pm 0.01$ (127.35)	$0.32 \pm 0.02$ (114.63)
5.5	$0.24 \pm 0.01$ (131.48)	$0.24 \pm 0.01$ (132.51)	$0.26 \pm 0.01$ (123.00)	$0.34 \pm 0.01$ (129.38)	$0.35 \pm 0.01$ (127.16)	$0.31 \pm 0.01$ (114.39)

<sup>a</sup>Carbon-13 chemical shifts (ppm).

into a spheroid-like morphology between generations 3 and 4. This is indicated in Figure 3, where the maximum asymmetry ( $I_z/I_x$ ) is plotted as a function of generation. We suggest that this occurs because these macromolecules (generation 4 and above) are able to effectively encapsulate the smaller guest molecules and hence decrease the measured  $T_1$ 's. This minimization of  $T_1$ 's does not

necessarily mean that the guest molecules are totally encapsulated; rather, they could be aggregated and congested at the surface of the polymer matrix. Thus we conclude that the suppressed  $T_1$  values ( $G = 3.5$ – $5.5$ ) are supportive of the extensive channeling and presence of interior void space predicted by the molecular dynamics simulations.

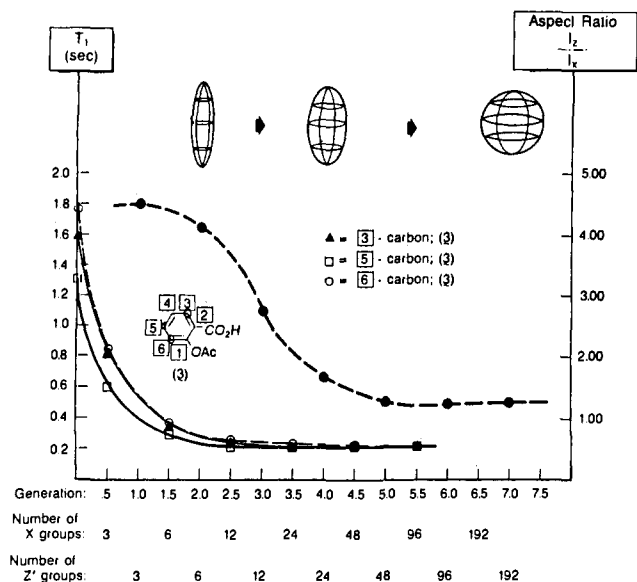


**Figure 3.** (Left axis): Comparison of carbon-13 spin-lattice relaxation times ( $T_1$ , s) vs generation for designated carbons (3, 5, and 6;  $\blacktriangle$ ,  $\square$ , and  $\circ$ , respectively) in **3** with  $\text{CHCl}_3$  solvent and various dendrimer generations. (Right axis): Molecular asymmetry ( $l/r$ ) vs dendrimer generation (number of  $Z'$  groups).

In conclusion, this work describes molecular simulations and physical measurements that suggest starburst branching strategies may be useful for controlling molecular morphogenesis.

**Acknowledgment.** We gratefully acknowledge useful discussions with Drs. D. M. Hedstrand and L. R. Wilson. The simulations were funded by a contract from Energy Conversion and Utilization Technologies Program of the Department of Energy. The computer equipment used was funded by a contract (No. N00014-86-K-0735) from Defense Advanced Research Projects Agency, Office of Naval Research, and by a grant (No. DMR-84-21119) from the Division of Materials Research of the National Science Foundation, Materials Research Groups.

Registry No. **3**, 94-75-7; **4**, 50-78-2.

### Synthesis and Crystal Structure of a Novel One-Dimensional Halogen-Bridged $\text{Ni}^{\text{III}}\text{-X-Ni}^{\text{III}}$ Compound, $\{[\text{Ni}(\text{R,R-chxn})_2\text{Br}]\text{Br}_2\}_\infty$

Koshiro Toriumi,\* Yoshiki Wada,<sup>1</sup> Tadaoki Mitani, and Shunji Bando

*Institute for Molecular Science  
Okazaki National Research Institutes  
Myodaiji, Okazaki 444, Japan*

Masahiro Yamashita\*

*College of General Education  
Nagoya University, Chikusa-ku, Nagoya 464, Japan*

Yuki Fujii

*Department of Chemistry, Faculty of Science  
Ibaraki University, Mito 310, Japan  
Received November 16, 1988*

Recently, the series of halogen-bridged  $\text{M}^{\text{II}}\text{-X-M}^{\text{IV}}$  mixed-valence compounds ( $\text{M} = \text{Pt}$ ,  $\text{Pd}$ , and  $\text{Ni}$ ) has attracted much interest from solid-state physicists and chemists as one-dimensional materials having strong electron-lattice interaction.<sup>2</sup> Their

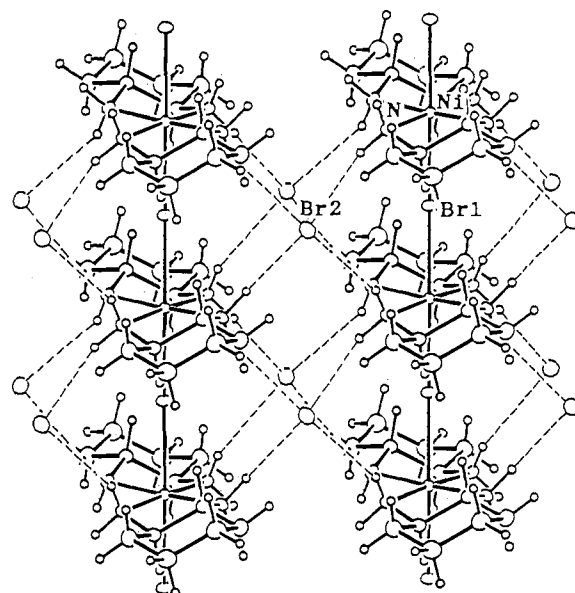


**Figure 1.** ORTEP drawing of a portion of the infinite chains along  $b$  with surrounding  $\text{Br}^-$  ions of  $\{[\text{Ni}(\text{R,R-chxn})_2\text{Br}]\text{Br}_2\}_\infty$  (**1**) at room temperature. The dashed lines correspond to hydrogen bonds. Thermal ellipsoids are 50% probability surfaces.

structures are well described as Peierls distorted linear chains with repeating unit  $\dots\text{M}^{\text{II}}\text{-X-M}^{\text{IV}}\text{-X}\dots$ , in which the Peierls distortion is defined by the displacement of the bridging halogen atom, X, from the midpoint between the two metal atoms toward the  $\text{M}^{\text{IV}}$  atom.<sup>2b</sup> They show characteristic physical properties, such as the strong intervalence charge-transfer absorption and the luminescence with large Stokes shift.<sup>2,3</sup> The solid-state properties can be interpreted by using an extended Peierls-Hubbard model which incorporates the electron-electron correlation on intermetal sites.<sup>4</sup> The relation between the Peierls energy gaps and lattice distortions for the compounds has been established by a number of structural<sup>5</sup> and optical studies.<sup>2b</sup> It is expected from this relation that a Ni system should be most suitable to prepare the  $\text{Ni}^{\text{III}}\text{-X-Ni}^{\text{III}}$  compound,<sup>6</sup> which is one extreme limit of the  $\text{M}^{\text{II}}\text{-X-M}^{\text{IV}}$  compound and is particularly interesting in its electronic structure and physical properties.<sup>7</sup>

We report here the synthesis, crystal structure, and physical properties of a novel bromo-bridged  $\text{Ni}^{\text{III}}\text{-X-Ni}^{\text{III}}$  linear chain compound with the (1*R*,2*R*)-cyclohexanediamine ligand,  $\{[\text{Ni}(\text{R,R-chxn})_2\text{Br}]\text{Br}_2\}_\infty$ . It is to our knowledge the first example of a halogen-bridged linear chain metal complex having no Peierls distortion.<sup>8</sup>

(3) (a) Clark, R. J. H. *Advances in Infrared and Raman Spectroscopy*; Heyden: London, 1984; Vol. 11, pp 95-132, and references therein. (b) Clark, R. J. H.; Kurmoo, M. *J. Chem. Soc., Faraday Trans. 2* **1983**, *79*, 519-527. (c) Tanaka, M.; Kurita, S.; Okada, Y.; Kojima, T.; Yamada, Y. *Chem. Phys.* **1985**, *96*, 343-348. (d) Tanino, H.; Koshizuka, N.; Kobayashi, K.; Yamashita, M.; Hoh, K. *J. Phys. Soc. Jpn.* **1985**, *54*, 483-486.

(4) (a) Nasu, K. *J. Phys. Soc. Jpn.* **1983**, *52*, 3865-3873. (b) Nasu, K. *Ibid.* **1984**, *53*, 302-311. (c) Nasu, K. *Ibid.* **1984**, *53*, 427-437.

(5) (a) Keller, H. J. *Extended Linear Chain Compounds*; Miller, J. S., Ed.; Plenum: New York, 1982; Vol. 1, pp 357-407, and references therein. (b) Endres, H.; Keller, H. J.; Martin, R.; Gung, H. N.; Traeger, U. *Acta Crystallogr., Sect. B* **1979**, *B35*, 1885-1887. (c) Beauchamp, A. L.; Layek, D.; Theophanides, T. *Ibid.* **1982**, *B38*, 1158-1164. (d) Yamashita, M.; Toriumi, K.; Ito, T. *Acta Crystallogr. Sect. C* **1985**, *C41*, 876-878. (e) Yamashita, M.; Ito, H.; Toriumi, K.; Ito, T. *Inorg. Chem.* **1983**, *22*, 1566-1568. (f) Toriumi, K.; Yamashita, M.; Ito, H.; Ito, T. *Acta Crystallogr., Sect. C* **1986**, *C42*, 963-968. (g) Clark, R. J. H.; Croud, V. B. *Inorg. Chem.* **1986**, *25*, 1751-1756. (h) Toriumi, K.; Yamashita, M.; Murase, I. *Chem. Lett.* **1986**, 1753-1754.

(6) (a) Yamashita, M.; Nonaka, Y.; Kida, S.; Hamaue, Y.; Aoki, R. *Inorg. Chim. Acta* **1981**, *52*, 43-46. (b) Yamashita, M.; Ito, T. *Ibid.* **1984**, *87*, L5-L7. (c) Yamashita, M.; Murase, I.; Ito, T.; Ikemoto, I. *Chem. Lett.* **1985**, 1133-1136. (d) Yamashita, M.; Murase, I. *Inorg. Chim. Acta* **1985**, *97*, L43-L44. (e) Toriumi, K.; Kanao, T.; Umetsu, Y.; Ohyoshi, A.; Yamashita, M.; Ito, T. *J. Coord. Chem.* **1988**, *19*, 209-221.

(7) Whangbo, M.-H.; Foshee, M. J. *Inorg. Chem.* **1981**, *20*, 113-118, and references therein.

(1) Present address: National Institute for Research in Inorganic Materials, Tsukuba, Ibaraki 305, Japan.

(2) (a) Tanino, H.; Kobayashi, K. *J. Phys. Soc. Jpn.* **1983**, *52*, 1446-1456. (b) Wada, Y.; Mitani, T.; Yamashita, M.; Koda, T. *Ibid.* **1985**, *54*, 3143-3153.